JST: Smart Systems and Devices
Volume 34, Issue 3, September 2024, 060-068

Motion Control of an Electric Power-Assisted Bicycle under the Effects of Operating Conditions

Bui Thu Huyen, Nguyen Ba Hung*
Hanoi University of Science and Technology, Ha Noi, Vietnam
** Corresponding author email: hung.nguyenba1@hust.edu.vn*

Abstract

The use of electric bicycle (EB) is considered as a useful solution for reducing the exhaust emissions and dependence of fossil fuels. Along with the development of EBs, studies on their motion characteristics have been receiving more attentions. In this paper, the control of the angular speed of the wheel in an electric power-assisted bicycle (EPAB) is discussed, considering external factors such as slope grade and wind speed. One proposed strategy to optimize vehicle speed is the particle swarm optimization (PSO) algorithm. To achieve this, a simulation model was developed to represent the operation of EPAB under rider control. Based on this operating model, mathematical models including a dynamic model of a bicycle under the driver's control, a dynamic model of an electric motor, and a vehicle speed control model using PSO - based proportional integral derivative (PID) controller are established. The simulation demonstrates that the PSO and PID controller is superior in terms of control compared to using it without PSO, and it works quickly in finding K_p, K_i, K_d to control the angular velocity of the wheel when external conditions change. These simulation results can also serve as useful resources for researchers looking to develop EPABs.

Keywords: EB, PID, PSO, slope grade, wind speed.

1. Introduction

During the past 100 years, the Earth's temperature has increased by nearly 1 degree [1]. This is partly due to the increase in greenhouse gases, particularly carbon dioxide (CO_2) emissions. Specifically, transportation is responsible for approximately one-fifth of global CO_2 emissions [2]. To minimize this impact, one important solution is the use of electric bicycles (EBs). An EB is a vehicle produced in the combination of a bicycle with the additional electric components such as electric motor, torque sensor, and control parts. EBs can be used even when the power is out or there are no electrical parts, however, when the power is on, the rider's power is reduced [3]. EBs are cost-effective and do not require road tax or insurance. EBs are a compact and flexible mode of transportation that can help reduce traffic congestion in large cities.

EBs are typically categorized into three main types: pure EBs, electric power-assisted bicycles (EPABs), and EBs that combine features of both pure electric and power-assisted bicycles. [4]. A pure EB is a type of bicycle that operates solely through the use of a control stick on the steering wheel. This control stick transfers electrical energy from the battery to the motor, allowing the bicycle to move without the need for pedaling. The pure EB is equipped with electric motors on the wheels or chassis. The pedals can be used when the power runs out. EPAB is equipped with a sensor that can detect pedal speed, pedal force, or both, and then transmits a voltage signal to a controller. The controller is responsible for controlling the electric motor to provide assistance to the rider while they are riding. The electric motor is typically installed on either the wheel hub or the chassis. The third type is a combination of pure electric and power-assisted modes, with two optional modes that are suitable for external conditions and the driver's preferences [5]. In addition, the type of EB can be determined by the location of the electric motor, which can be placed on the front wheel axle, in the middle (near the pedal shaft), or on the rear wheel shaft. Placing the motor on the front wheel axle can improve force distribution, but it may also cause wheel slippage on steep terrain. The mid-mounted motor is small and easy to integrate into the frame, but it is complex and difficult to maintain. If it becomes damaged, the entire assembly must be replaced, resulting in high costs. On the other hand, placing the motor on the rear wheel axle can create imbalance and put excessive pressure on the rear wheel. However, it offers better acceleration and prevents wheel slippage compared to placing the motor on the front wheel axle.

Among EBs, electric assist bicycles are gaining significant attention from users and research organizations. These bicycles not only have the aforementioned advantages, but they also promote physical exercise and strength [6]. Therefore, this

ISSN 2734-9373
https://doi.org/10.51316/jst.176.ssad.2024.34.3.8
Received: Jun 5, 2024; revised: Jul 24, 2024,
accepted: Aug 2, 2024

paper will focus on electric power-assisted bicycles. Nowadays, the proportional integral derivative (PID) controller is commonly used in industrial systems due to its efficient control capabilities, simple design, and wide range of applications. There are many methods available for calibrating the parameters of the PID controller. However, for certain systems, the calibration process can be time-consuming and challenging due to the influence of noise and errors on the measurement signal. This can make it difficult to achieve optimal values for the PID controller. In such cases, PID calibration methods can be combined with algorithms such as particle swarm optimization (PSO), which is considered an optimal control method [7].

Ukan Uyar *at el*. [8] conducted simulations and experiments to evaluate the effectiveness of a new drive mechanism and intelligent control system in regulating the speed of an EB. The performance of various algorithms is compared, including PI, PID, Fuzzy PID, and Hybrid Fuzzy. The results showed that the Hybrid Fuzzy and FPID3 controllers were similar in terms of timing analysis parameters and performance criteria, but were more successful than traditional controllers. However, the use of a PSO-based PID controller has not yet been implemented. The PSO algorithm has attracted a great deal of attention from researchers and has been used successfully in various fields. Arkadiusz Ambrozial *at el*. [9] presents a method for optimising the settings of a PID controller for an air handling unit equipped with many actuators with different parameters. After implementing the module, no further errors were encountered and the control quality, as measured by integration quality factors, improved by an average of 64%. S. Ahmadi *at el*. [10] studied an effective method based on the combination of a PSO algorithm and a proposed PID controller (PSO-PID) for maximum power point tracking (MPPT) of proton exchange membrane (PEM) fuel cells. As a result, the PSO algorithm with fast convergence, high accuracy and very low power fluctuations tracks the maximum power point of the fuel cell system. However, there is currently no research on the implementation of a PSO-PID controller for speed control in EBs. Therefore, this paper aims to examine the topic mentioned above.

To achieve this, a mathematical model of an EB with driver support and a speed control model using a PSO-PID controller were established. The results of the speed control with and without the PSO-PID controller were compared. Additionally, the impact of slope grade and wind speed on the use of this controller is taken into consideration. The paper is divided into four parts: 1. Introduction, 2. Building mathematical models, 3. Simulation results, and 4. Conclusion.

2. Building Mathematical Models

2.1. Mathematical Model of a Bicycle with Rider's Control and Motor Assistance

To run the simulation, it is necessary to thoroughly examine the mathematical model. Fig. 1 illustrates the kinematic model of a cyclist's control and motor assistance while riding up a slope with a degree of α (°) in the coordinate system.

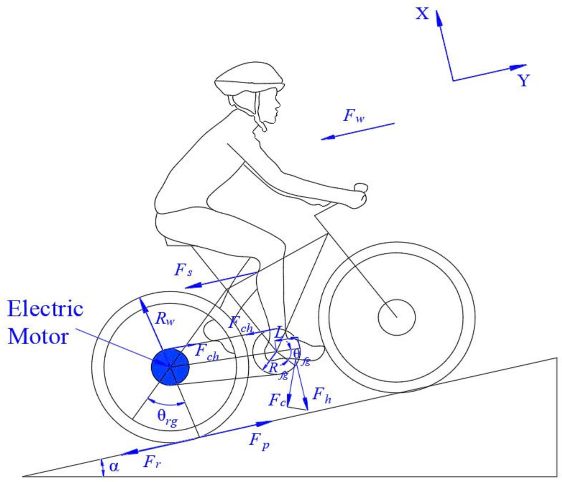

Fig. 1. Force analysis model of an EPAB

The forces acting on the bicycle and rider are represented according to Newton's Second Law:

$$\vec{F} = m\vec{a} \tag{1}$$

or:

$$F_p - (F_r + F_s + F_w) = Ma = \frac{d^2x}{dt^2} \tag{2}$$

where, F_p represents the propulsion force, F_r is the rolling resistance, F_s is the slope resistance, F_w is the wind resistance, M is the total mass of both the rider and the EB, a is the acceleration, t is the time, and x is the distance traveled by the EB in time t.

The calculation for rolling resistance is as follows:

$$F_r = 9.81MC_r.cos\alpha \tag{3}$$

where, C_r is the coefficient of rolling resistance and α is the slope angle in degrees. (°).

The slope resistance is determined by the angle of the slope:

$$F_s = 9.81M.sin\alpha \tag{4}$$

The resistance of the wind can be described as follows:

$$F_w = \frac{C_d.D.A.(v_w + v)^2}{2} \tag{5}$$

where, C_d is the drag coefficient, D is the air density (kg/m^3), A is the wind resistance area (m^2), v is the speed of the EB (m/s), and v_w is the wind speed (m/s).

In case of only human's power, the force of propulsion is determined by:

$$F_{po} = \frac{T_r}{R_w} \tag{6}$$

In this equation, R_w represents the radius of the EB in meters (m), T_r is the rider's torque (N.m).

When a human's power is combined with the assistance of an electric motor located on the rear wheel hub, the resulting propulsion force can be calculated by:

$$F_p.R_w = T_p = T_r + T_m \tag{7}$$

where, T_p is the propulsion torque (N.m), T_m is the torque supported by the electric motor which is assumed equal to the load torque acting on the shaft (N.m).

Based on Fig. 1, the rider's torque is defined as follows:

$$T_r = F_{ch}.R_{rg} \tag{8}$$

where, R_{rg} is the radius of the rear gear in meters (m), F_{ch} is the force applied to the chain. This force can be calculated by:

$$F_{ch} = \frac{1}{R_{fg}}.L.F_h.cos\theta_{fg} \tag{9}$$

where, L represents the crank length (m), F_h is the force exerted by the rider (N), and θ_{fg} is the rotation angle of the front gear.

From (7), (8), and (9), the propulsion force can be calculated:

$$F_p.R_w = \frac{1}{R_{fg}}.L.F_h.cos\theta_{fg}.R_{rg} + T_m$$

$$\rightarrow F_p = \frac{1}{R_w}.\frac{R_{rg}}{R_{fg}}.L.F_h.cos\theta_{fg} + \frac{T_m}{R_w} \tag{10}$$

The torque T_m can be calculated using the following equations:

$$L_m.\frac{di_m}{dt} + i_m.R_m + K_b.\omega_m = K_a.u \tag{11}$$

$$J_m.\frac{d\omega_m}{dt} + B_m.\omega_m + T_m = K_t.i_m \tag{12}$$

where, i_m, R_m, and L_m are the current, resistance and inductance of the motor, respectively; u is the input voltage. K_a is the amplification coefficient of motor driver; K_b is back-emf constant; B_m and J_m are the frictional coefficient and the moment of inertia, respectively.

The propulsion force can be deduced from (10), (11) and (12):

$$F_p = \frac{1}{R_w}.\frac{R_{rg}}{R_{fg}}.L.F_h.cos\theta_{fg} + \frac{K_t.i_m - J_m.\frac{d\omega_m}{dt} - B_m.\omega_m}{R_w}$$

$$\rightarrow F_p = \frac{1}{R_w}.\frac{R_{rg}}{R_{fg}}.L.F_h.cos\theta_{fg} + \frac{1}{R_w}.\left[\frac{K_t.K_a}{R_m}.u - \frac{K_t.L_m}{R_m}.\frac{di_m}{dt} - J_m.\frac{d\omega_m}{dt} - \left(B_m + \frac{K_t.K_b}{R_m}\right).\omega_m\right] \tag{13}$$

2.2. Required Power

The power needed to operate a bicycle is determined by the amount of resistance it must overcome, which includes factors such as wind resistance, friction, and slope resistance:

$$P = F.v \tag{14}$$

$$\rightarrow P = (F_f + F_s + F_w).v \tag{15}$$

In these equations, P is the required power (W), F is the resistance force acting on the bicycle (N), and v is the speed of the bike (m/s).

In the following formula, (3), (4), and (5) are combined to obtain the necessary power:

$$P = \left[9.81.M.(C_r\cos\alpha + G) + \frac{C_d.D.A.(v_w+v)^2}{2}\right] \tag{16}$$

where, G is the slope grade (%), which is calculated by: G = sinα with α is the slope angle (°)

2.3. Model-Based Control for Bicycle Speed Using PSO - Based PID Controller

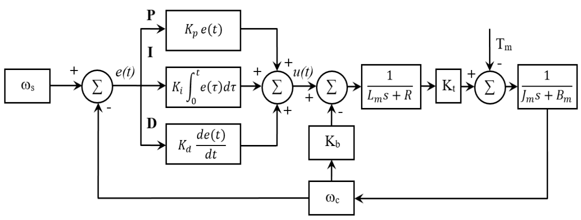

Fig. 2. Control model for EPAB angular velocity using PID algorithm

Fig. 2 illustrates the wheel angular velocity control model of an EPAB utilizing the PID algorithm, in which the voltage *u(t)* is used as a control variable which is described in (11). The PID algorithm consists of three fundamental coefficients: proportional, integral, and derivative, which are adjusted to reflect priority [11].

The proportional component is solely determined by the discrepancy between the set point and the process variable, which is known as the error term. The integral component calculates the cumulative error over time. The result is that even a small error term will cause a slow increase in the integral component. The derivative component causes the output to decrease when the process variable is increasing rapidly. The derivative response is directly proportional to the rate of change of the process variable.

PSO is a method for optimizing complex numerical functions, originally developed by Kennedy and Eberhart [12]. Fig. 3 shows the PSO algorithm flowchart. It is based on the concept of social behavior observed in flocks of birds and schools of fish. A swarm is made up of individuals, known as particles, that continuously alter their positions. Each individual particle represents a potential solution to the problem. Particles fly around in a multi-dimensional search space, adjusting their positions based on their own experiences and those of their neighboring particles. They utilize the best position they have encountered, both individually and collectively with their neighbors [13].

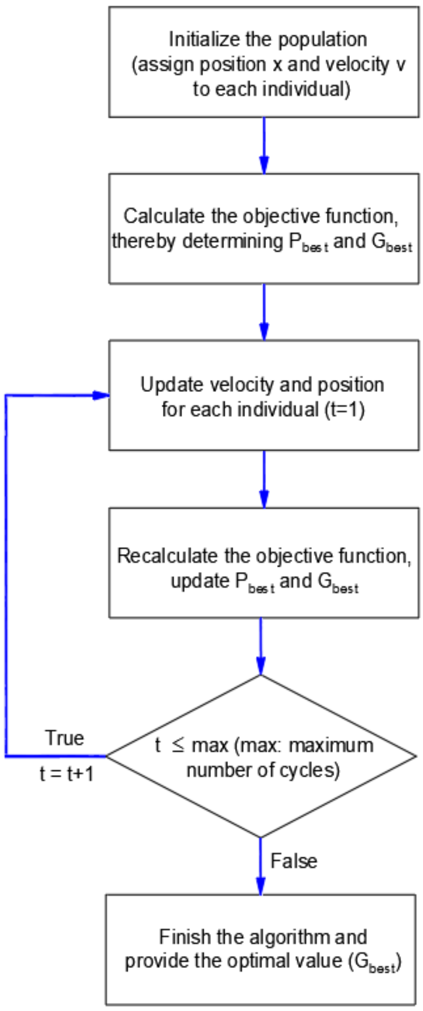

Fig. 3. PSO algorithm flowchart

In order to update elements, the following formulas are used [14]:

$$v_{i,m}^{(t+1)} = w.v_{i,m}^{(t)} + c_1.rand().(P_{best_{i,m}} - x_{i,m}^{(t)}) + c_2.rand().(G_{best_{i,m}} - x_{i,m}^{(t)}) \quad (17)$$

$$x_{i,m}^{(t+1)} = x_{i,m}^{(t)} + v_{i,m}^{(t+1)}$$
$$i = 1, 2, \ldots, n \quad (18)$$
$$m = 1, 2, \ldots, d$$

In these formulas, x_i^k is the current location, x_i^{k+1} is the changed location, v_i^k is the current velocity, v_i^{k+1} is the changed location, P_{best_i} is the best position for the *i*-th individual, G_{best_i} is the best element of the individual *i*-th in the population, v_i^{Gbest} is is velocity according to G_{best}, v_i^{Pbest} is velocity according to P_{best}, *n* is the number of swarms, *d* is population size, *t* is the number of repetitions; $v_{i,m}^{(t)}$ is the speed of the *i*-th element at repetition, *w* is the inertia coefficient; c_1, c_2 are the acceleration coefficients; *rand( )* is a random number in the range (0,1); $x_{i,m}^{(t)}$ is the sampling position of the *i*-th element in the *t*-th iteration.

3. Simulation Results

3.1. Control the Wheel Angular Speed of EPAB Using PSO-Based PID Controller

Fig. 4 shows the sum of squared errors versus number of iterations for the EB control system of the PSO - based PID controller. It turns out that the more iterations are performed, the smaller the total error is. This is because after each iteration, the instance is updated with its position and the evaluation of the objective function value, whereby the best value that the instance has ever achieved is updated. The EB is controlled at angular speed of the wheel ω = 25 rad/s with input parameters: M_r = 60 kg, M_b = 25 kg, L = 0.17 m, R_w= 0.27 m, G = 0%, and v_w = 0 m/s. EPAB is controlled by setting the angular speed of the wheel to ω_s = 25 rad/s. However, when the PID parameters are not optimized (with K_p = 1, K_i = 1, K_d= 1), the wheel's angular speed rapidly increases and overshoots to nearly 35 rad/s before gradually decreasing and fluctuating around 25 rad/s, eventually stabilizing (as shown in Fig. 5). On the other hand, when using the PSO-PID controller with optimized parameters (K_p = 0.556, K_i = 0.011, K_d = 0.051), the angular speed of the wheel reaches 25 rad/s. Although it does not increase as quickly as when not in use, it also does not overshoot, thus avoiding energy loss. Once the desired speed is achieved, the vehicle maintains a stable speed.

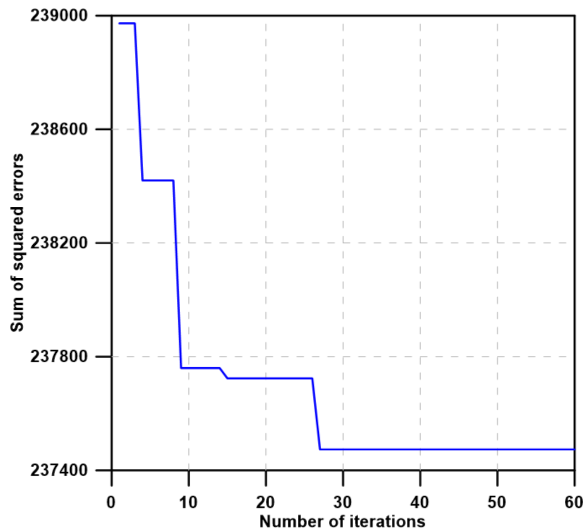

Fig. 4. Sum of squared errors versus number of iterations

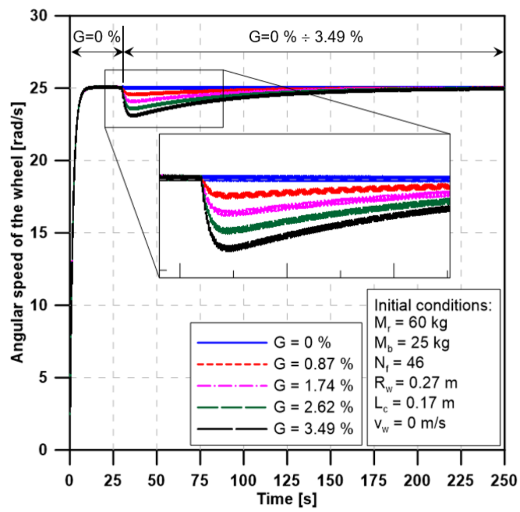

Fig. 6. Influences of slope grade on the controlled angular speed of the wheel

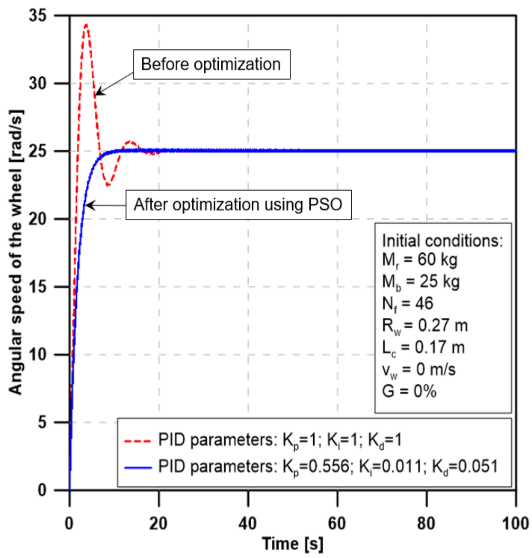

Fig. 5. Controlled angular speed of the wheel at the set value ω_s=25 rad/s

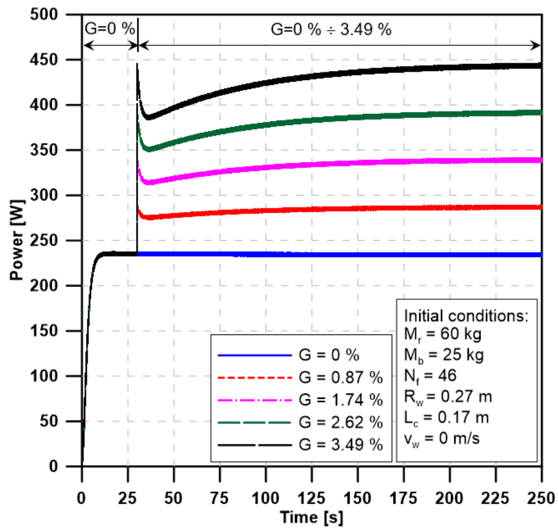

Fig. 7. Influences of G on the power of EPAB

3.2. Effect of Slope Grade

Slope is a significant factor that affects control performance. It is evaluated based on the input conditions shown in Fig. 6 and Fig. 7. In the first 30 seconds, with G = 0%, the running speed increases rapidly and then stabilizes (as shown in Fig. 6). However, after 30 seconds, the slope changes from 0% to 3.49%, and the wheel's angular speed starts to have an impact. As the slope becomes steeper, the slope resistance increases, thus the propulsion force decrease, resulting in a decrease in angular speed of the wheel. With the help of the controller, the speed gradually increases and stabilizes at 200 seconds.

As the slope increases, the angular speed of the wheel decreases, which leads to a sudden increase in power to maintain the desired speed. After that, the power is no longer sufficient to overcome the slope resistance for a short time, thus the power decreases, and the velocity also decreases accordingly at this point. Specifically, the power drops to 236.56 W, 392.53 W (corresponding to G = 0.87% and G = 3.49%). The power then increases again to maintain the set angular speed of the wheel (see Fig. 7). If the slope is greater, the power increases more sharply. Fig. 8 shows the max power of the EPAB when the slope grade increases from 0% to 3.49%, in which the max power at G = 0% is 235.49 W and at G = 3.49% is 444.5 W, which corresponds to an increase of 35.68%. This is due to the fact that more energy is required to maintain a set angular speed of the wheel.

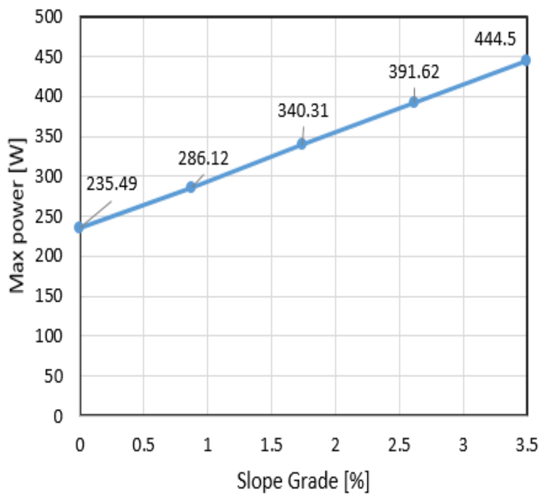

Fig. 8. Influences of G on the max power

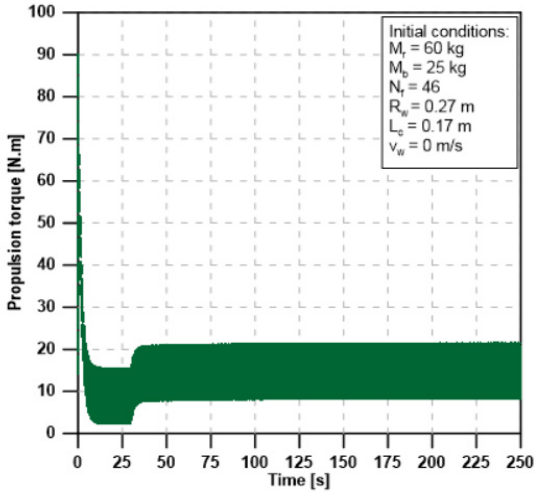

Fig. 11. The propulsion torque when $G = 2.62\%$

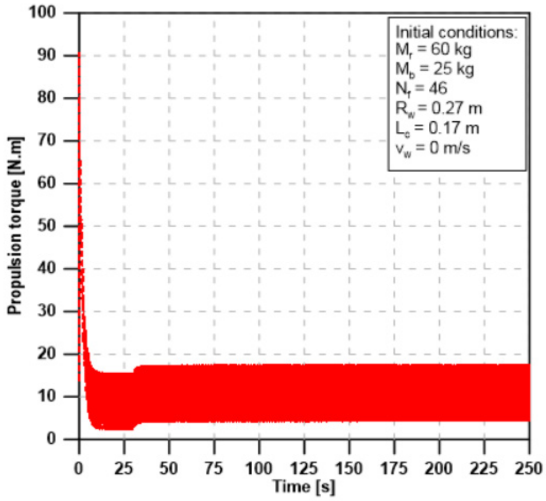

Fig. 9. The propulsion torque when $G = 0.87$ %

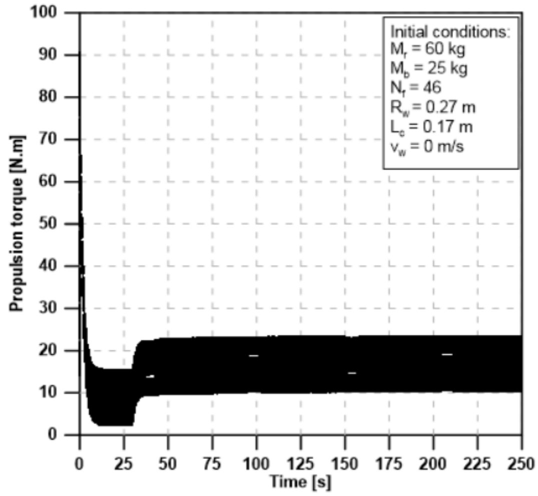

Fig. 12. The propulsion torque when $G = 3.49$ %

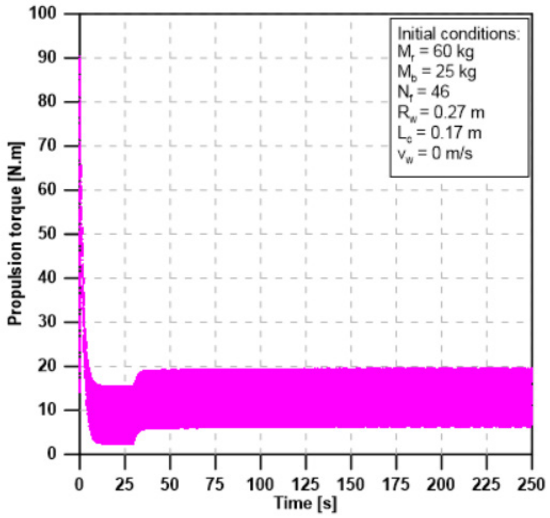

Fig. 10. The propulsion torque when $G = 1.74$ %

Fig. 9 to Fig. 12 show the propulsion torque when G is 0.87%, 1.74%, 2.62% and 3.49% respectively. At the beginning, when the slope is 0%, the propulsion torque increases rapidly to 90.55 N.m. After reaching a stable angular speed of the wheel, the propulsion torque decreases rapidly and is range from 2.3 N.m to 15.16 N.m for 30 seconds. After applying the slope factor, the propulsion torque increases to maintain the required angular speed of the wheel. When the slope is greater, the propulsion torque increases more, corresponding to G of 0.87% - 3.49%, the average propulsion torque is 10.83 N.m, 12.75 N.m, 14.68 N.m and 16.61 N.m respectively.

3.3. Effect of Wind Speed

When riding, wind speed is an important factor to consider. In this study, the wind speed is evaluated on a scale of 0 to 5 m/s, with the input conditions shown in Fig. 13 and Fig. 14. It is observed that during the first 30 seconds, when the wind speed is at 0 m/s, the angular speed of the wheel increases rapidly and then stabilizes. However, after 30 seconds, the wind speed changes to 5 m/s, which has an impact on the velocity. As the wind speed increases, the wind resistance on the EPAB decreases, resulting in a decrease in the angular speed of the wheels. With the help of the controller, the speed gradually increases and stabilizes at 200 seconds.

As the wind speed increases from 0 m/s to 5 m/s, the angular velocity of the wheel decreases due to the sudden increase of the wind resistance force in a short phase. As the result, the power suddenly increases just after the wind speed is activated from 1 m/s to 5 m/s, and then it reduces because of the reduction of the wheel angular velocity as described above. At a wind speed of 1 - 5 m/s, the lowest powers at these points are 277.35 W, 323.17 W, 369.96 W, 416.89 W and 462.99 W, respectively. The power then increases again to maintain the set angular velocity of the wheel, as observed in Fig. 14. The higher the wind speed, the higher the power, as more energy is required to maintain the set angular velocity of the wheel. Fig. 15 shows the maximum power of the EPAB when the wind speed increases from 0 m/s to 5 m/s. At a wind speed of 0 m/s, the maximum power is 235.49 W and at a wind speed of 5 m/s, the maximum power is 609.23 W, which corresponds to an increase of 61.35 %.

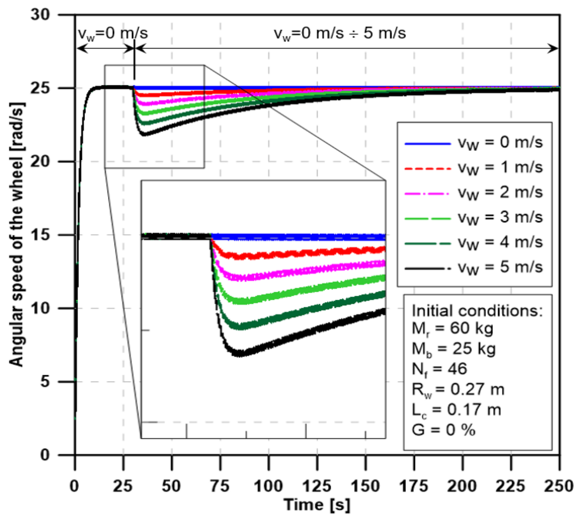

Fig. 13. Influences of wind speed on the controlled angular speed of the wheel

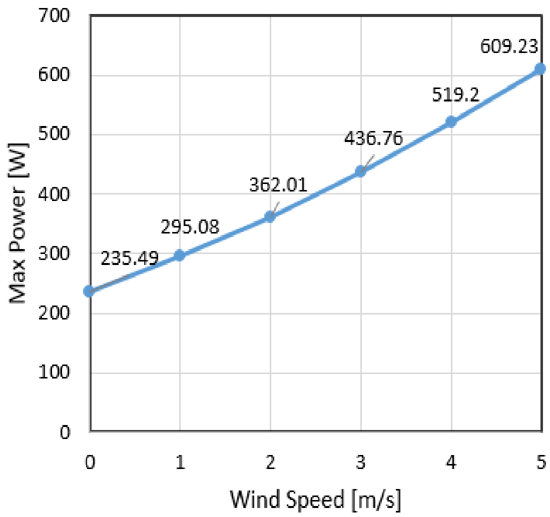

Fig. 15. Influences of wind speed on the max power

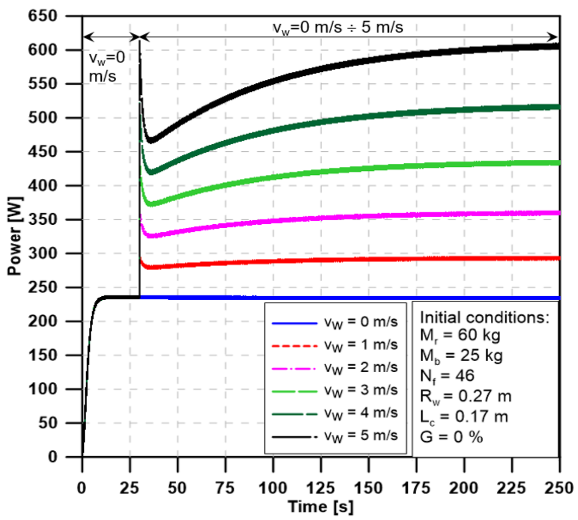

Fig. 14. Influences of wind speed on the power of EPAB

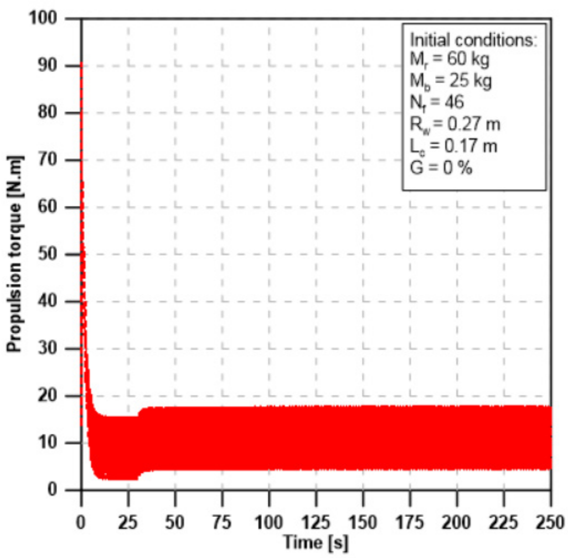

Fig. 16. The propulsion torque when v_w = 1 m/s

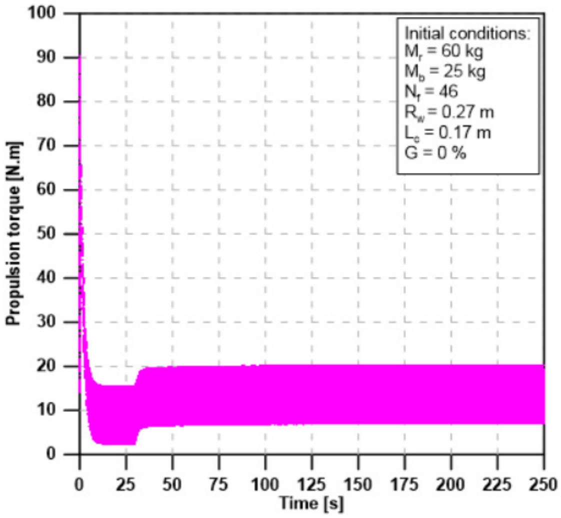

Fig. 17. The propulsion torque when v_w = 2 m/s

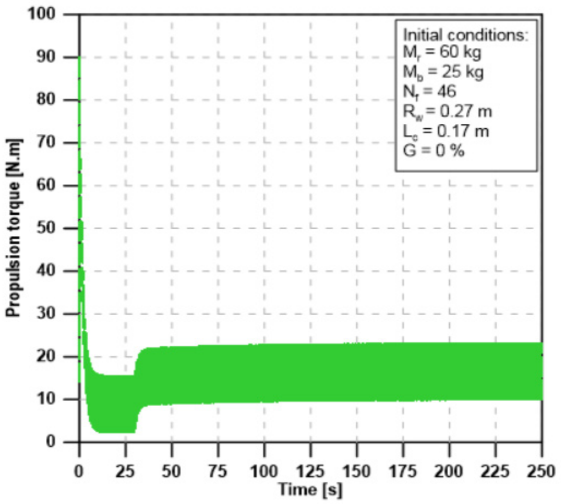

Fig. 18. The propulsion torque when v_w = 3 m/s

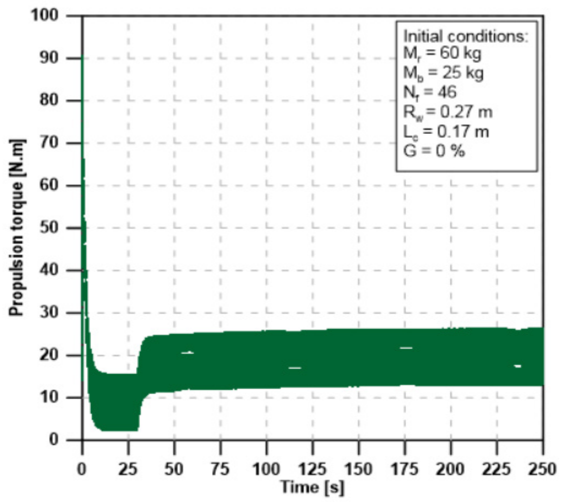

Fig. 19. The propulsion torque when v_w = 4 m/s

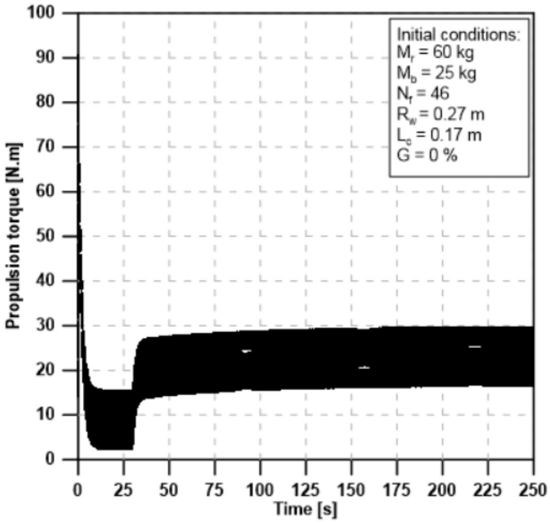

Fig. 20. The propulsion torque when v_w = 5 m/s

Fig. 16 to Fig. 20 show the propulsion torque when the wind speed increases from 1 - 5 m/s. When the wind speed is still 0 m/s, to reach a stable speed, the propulsion torque quickly increases to 90.55 N.m. Then the propulsion torque decreases rapidly and fluctuates within a fixed range for 30 seconds. However, as the wind speed increases, the propulsion torque increases to maintain the required angular velocity of the wheel. As the gradient increases, the thrust torque increases. When the wind speed is 0 m/s, the average thrust torque is 8.9 N.m. When the wind speed is varied at 1 m/s, 2 m/s, 3 m/s, 4 m/s, and 5 m/s, the average propulsion torque obtains 11.05 N.m, 13.47 N.m, 16.16 N.m, 19.11 N.m, and 22.31 N.m, respectively. The corresponding increase compared to the propulsion torque at a wind speed of 0 m/s is 19.46%, 33.93%, 44.93%, 53.43%, 60.11%.

4. Conclusion

A study was conducted to control the angular velocity of the wheel using the PID tuning method in combination with PSO algorithm. The simulation results showed that the angular velocity of the wheel with only using PID controller was not as well controlled as with the combination of PID and PSO. In addition, the speed of the EPAB decreased when the slope changed from 0% to 3.49% and the wind speed changed from 0 m/s to 5 m/s, but thanked to the controller, the angular velocity of the wheel was precisely controlled to the target value. Similarly, when the slope and wind speed were increased, the propulsion torque increased and oscillated within a certain range. Besides, the power of EPAB increased and tended to a stable value. Specifically, when the slope was 3.49%, the EPAB power increased by 35.68% compared to a slope of 0%, and when the wind speed was 5 m/s, the power increased by 61.35% compared to a wind speed of 0 m/s.

From the above simulations, it was found that the PSO and PID controller worked quickly in the search of K_p, K_i, K_d to control the angular velocity of the wheel when the external conditions were changed. This study could be a useful document for researchers to improve the control performance of motion for EPABs.

References

[1] M. Kovacikova, P. Janoskova, K. Kovacikova, The impact of emissions on the enviroment within the digital economy, Transportation Research Procedia, vol. 55, Jul. 2021, pp. 1090-1097. https://doi.org/10.1016/j.trpro.2021.07.080

[2] H. Ritchie, Cars, planes, trains: where do CO2 emissions from transport come from?, Our world in data, Oct. 6, 2020. [Online]. Available: https://ourworldindate.org/co2-emissions-from-transport

[3] A. Ramadhan, R. Dinata, Development of electric bicycle and its impact on the environment, IOP Conference Series: Materials Science and Engineering, vol. 1122, Apr. 2021, pp. 012054. https://doi.org/10.1088/1757-899X/1122/1/012054

[4] A. Muetze, Y.C. Tan, Modeling and analysis of the technical performance of DC-motor electric bicycle drives based on bicycle road test data, IEEE Conference, Antalya, Turkey, May. 3-5, 2007, pp. 1574-1581. https://doi.org/10.1109/IEMDC.2007.383663

[5] N. B. Hung, O. Lim, A review of history, development, design and research of electric bicycles, Applied Energy, vol. 260, Feb. 2020, pp. 114323. https://doi.org/10.1016./j.apenergy.2019.114323

[6] A. Riiser, E. Beer, L. B. Anderden, S. Nordengen, E-cycling and health benefits: A systematic literature review with meta - analyses, Frontiers in Sports and Active Living, vol. 4, Oct. 2022, pp.10311004. https://doi.org/10.3389/fspor.2022.1031004

[7] Z. Gaining, A particle swarm optimization approach for optimum design of PID controller in AVR system, IEEE Transactions on Energy Conversion, vol. 19, no.2, pp. 384 - 391, Jun. 2004. https://doi.org/10.1109/TEC.2003.821821

[8] O. Uyar, M. Cunkas, H. Karaca, Enhanced intelligent control with adaptive system for electrically assisted bicycle, Engineering Science and Technology, an International Journal, vol. 30, Jun. 2022, pp. 101047 https://doi.org/10.1016/j.jestch.2021.08.004

[9] A. Ambroziak, A. Chojectki, The PID controller optimisation module using fuzzy self - tuning PSO for air handling unit in continuous operation, Engineering Applications of Artificial Intelligence, vol. 117, Jan. 2023, pp. 105485. https://doi.org/10.1016/j.engappai.2022.105485

[10] S. Ahmadi, Sh. Abdi, and M. Kakavand, Maximum power point tracking of a proton exchange membrane fuel cell system using PSO-PID controller, International Journal of Hydrogen Energy, vol. 42, Aug. 2017, pp. 20430 - 20443. https://doi.org/10.1016/j.ijhydene.2017.06.208

[11] R. Borase, D. K. Maghade, S.Y. Sondkar, and S. Pawar, A review of PID control design, tuning methods and applications, International Journal of Dynamics and Control, vol. 9, Jul. 2020, pp. 818-827. https://doi.org/10.1007/s40435-020-00665-4

[12] J.Kennedy, R. Eberhart, Particle swarm optimization, Proceedings of ICNN'95 - International Conference on Neural Networks, Perth, WA, Australia, Nov. 27 - Dec. 01, 1995, pp. 1942-1948. https://doi.org/10.1109/ICNN.1995.488968

[13] H. Fan, A modification to particle swarm optimization algorithm, Engineering Computations, vol. 19, no. 8, Jul. 2002, pp. 970 - 989. https://doi.org/10.1108/02644400210450378

[14] T. J. Su, H. C. Wang, and J. W. Liu, Particle Swarm Optimization for Image Noise Cancellation, Third International Conference on Intelligent Information Hiding and Multimedia Signal Processing, Kaohsiung, Taiwan, Nov. 26-28, 2007. https://doi.org/10.1109/IIH-MSP.2007.237